Supporting information

Insight into the effect of copper substitution on the catalytic performance of $LaCoO_3$-based catalysts for direct epoxidation of propylene with molecular oxygen

Jianyi Lei,[a] Jiajun Dai,[a] Kok Bing Tan,[a] Jiale Huang, [a]* Guowu Zhan,[b]* Qingbiao Li[a,c]

[a] *Department of Chemical and Biochemical Engineering, College of Chemistry and Chemical Engineering, and National Laboratory for Green Chemical Productions of Alcohols, Ethers and Esters, Xiamen University, Xiamen 361005, P. R. China*

[b] *College of Chemical Engineering, Huaqiao University, Xiamen 361021, P. R. China*

[c] *College of Food and Biology Engineering, Jimei University, Xiamen, Fujian 361021, P. R. China*

*Corresponding authors
E-mail address: cola@xmu.edu.cn (J. Huang), gwzhan@hqu.edu.cn (G. Zhan).

Number of pages: 16
Number of figures: 9
Number of tables: 3

Table of Contents

Supporting Figures

Supporting Tables

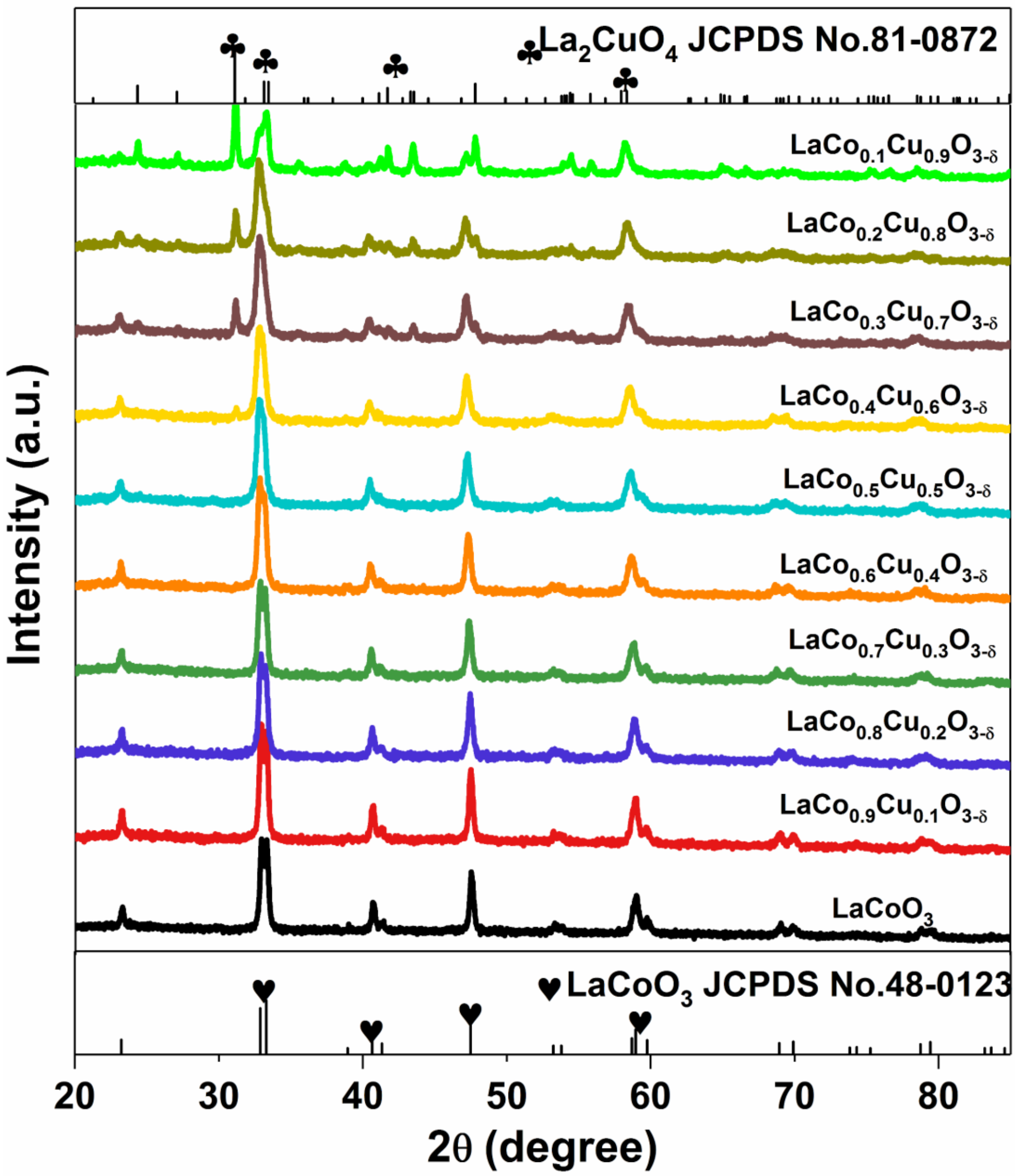

Figure S1. The XRD patterns of different copper doping on $LaCoO_3$

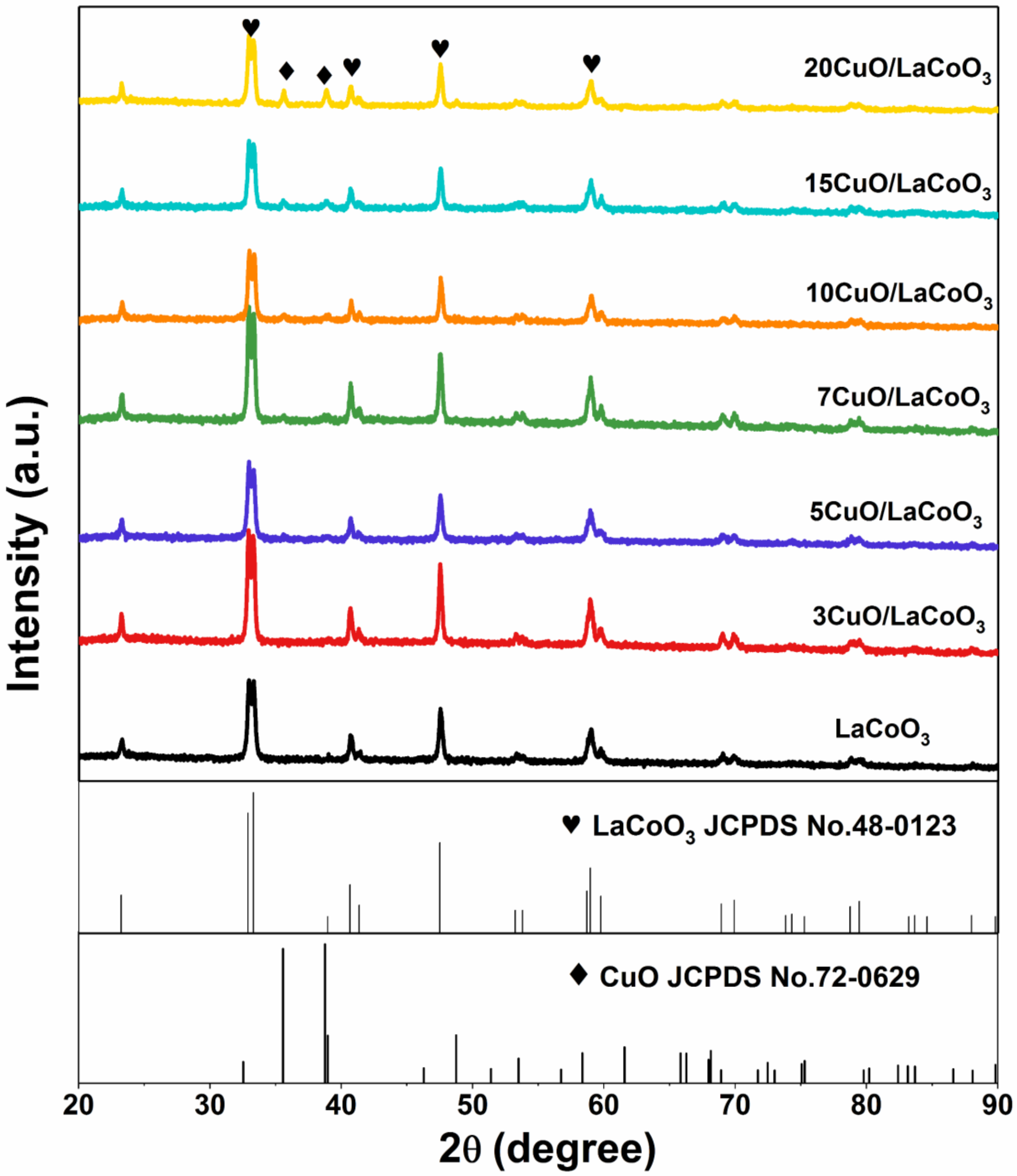

Figure S2. The XRD patterns of different copper oxide loading on $LaCoO_3$

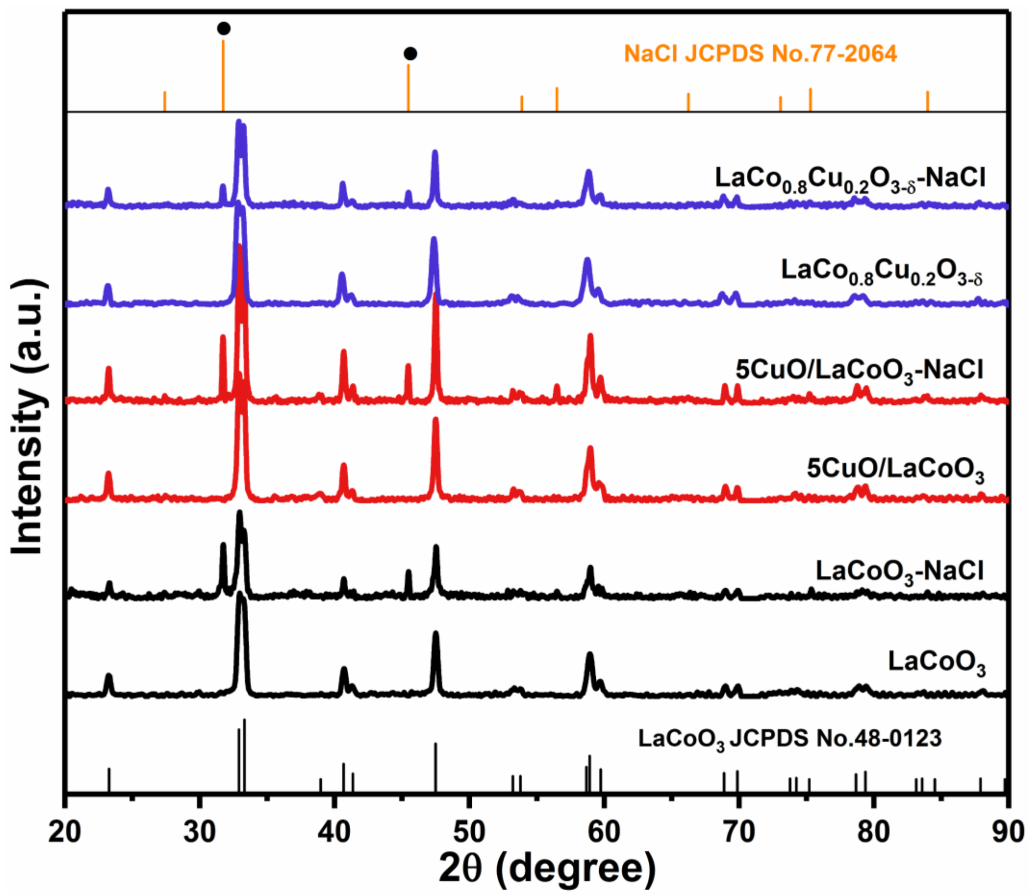

Figure S3. The XRD patterns of representative samples with and without NaCl modication. (The concentration of NaCl solution is 0.0256 M)

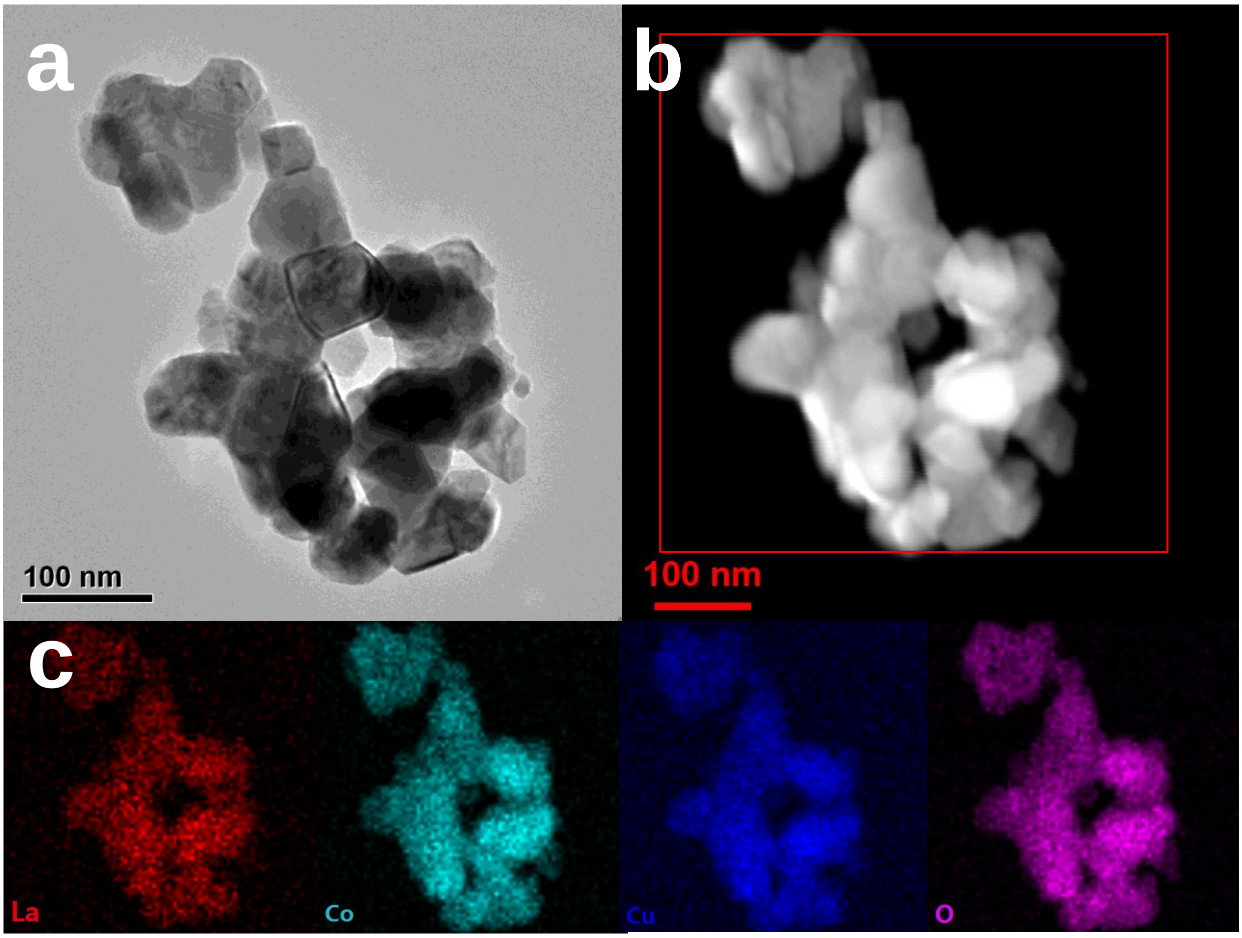

Figure S4. (a) Representative TEM image and (b-c) corresponding EDX elemental maps of $LaCo_{0.8}Cu_{0.2}O_{3-\delta}$-NaCl sample (Only describing La, Co, Cu, and O since NaCl is hardly to be detected after ultrasonic process for $LaCo_{0.8}Cu_{0.2}O_{3-\delta}$ sample promoted with NaCl.

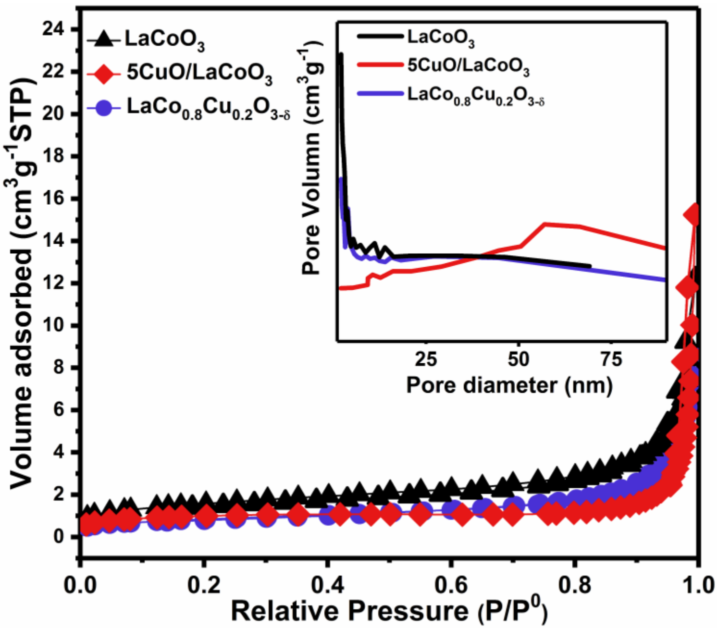

Figure S5. N_2 adsorption/desorption isotherms with insert of pore size distribution of representative samples;

Cu doping $LaCoO_3$ perovskites exhibit poor N_2-adsorption ability as compared to pure $LaCoO_3$, as well as the decrease of specific surface area (only 3.033 m^2g^{-1}). Since the surface area of $LaCoO_3$ synthesized by chemical sol-gel method is proven to be relatively low (5.649 m^2g^{-1} in this study), $LaCo_{0.8}Cu_{0.2}O_{3-\delta}$ perovskites remain physically inert, indicating its similar textural properties to $LaCoO_3$ perovskites prepared by conventional chemical method. This was also confirmed by pore diameter distribution curves inside. Even addition with CuO, the materials still show low surface area and weak adsorption but more average pore diameter distribution owing to formation of CuO aggregates. These results demonstrated that perovskites materials in this study are nonporous or microporous and corresponding mainly to type II of the IUPAC classification.[1] Furthermore, the curves of pore diameter distribution of $LaCoO_3$ and $LaCo_{0.8}Cu_{0.2}O_{3-\delta}$ are almost consistent which testify that both of these two samples possess a classical perovskite structure and hardly formation of CuO particles for the $LaCo_{0.8}Cu_{0.2}O_{3-\delta}$ sample , matching well with the results of XRD results.

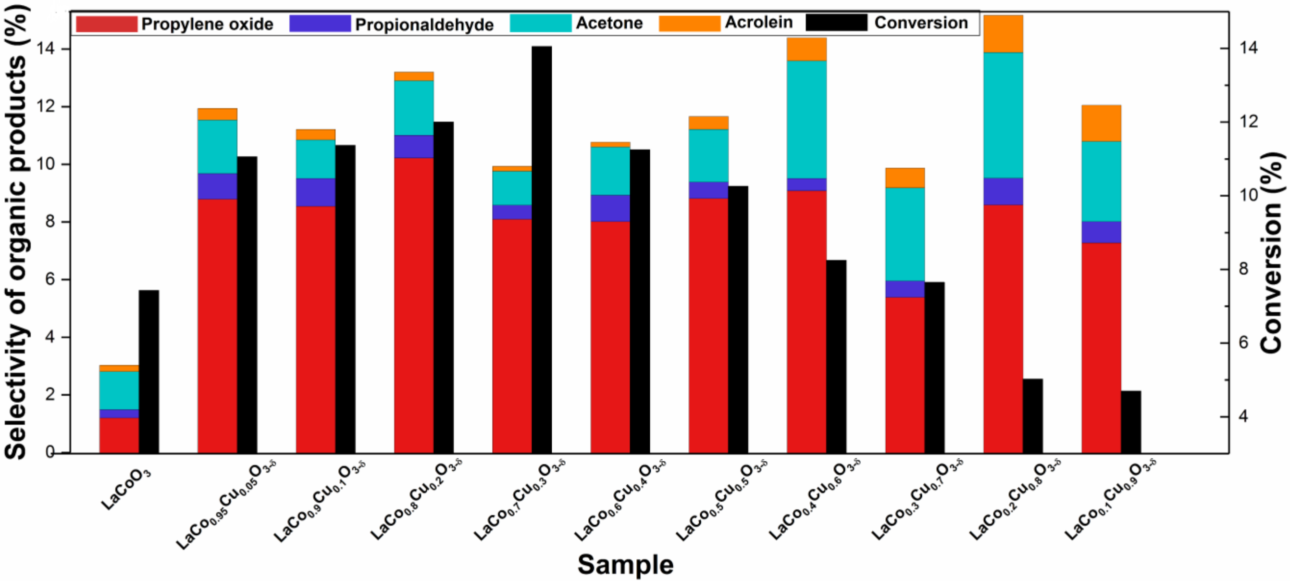

Figure S6. Distribution of organic products over $LaCo_xCu_{1-x}O_{3-\delta}$ catalysts and corresponding propylene conversion (all samples were modified with NaCl solution with a concentration of 0.0256 M).

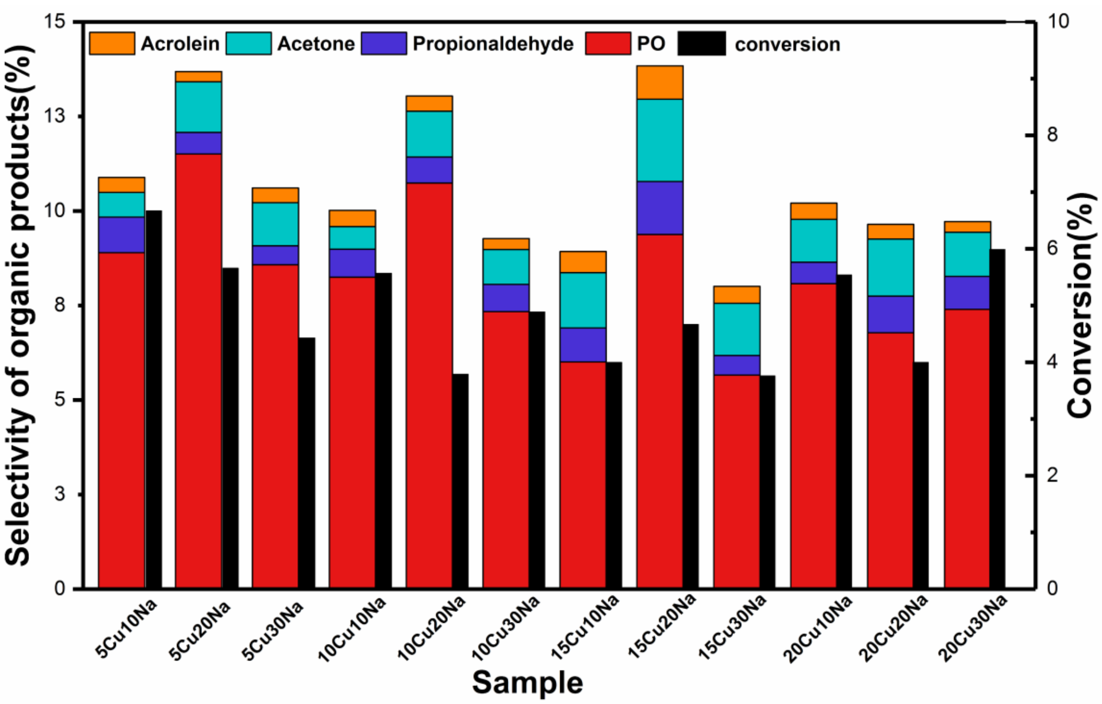

Figure S7. Distribution of organic products over $xCuO/LaCoO_3$-yNaCl catalysts and corresponding propylene conversion (where x represents the nominal content (wt. %) of copper on the $LaCoO_3$, y represents the mass ratio of NaCl to $xCuO/LaCoO_3$ used in NaCl solution, corresponding to 0.0128-0.0384 M).

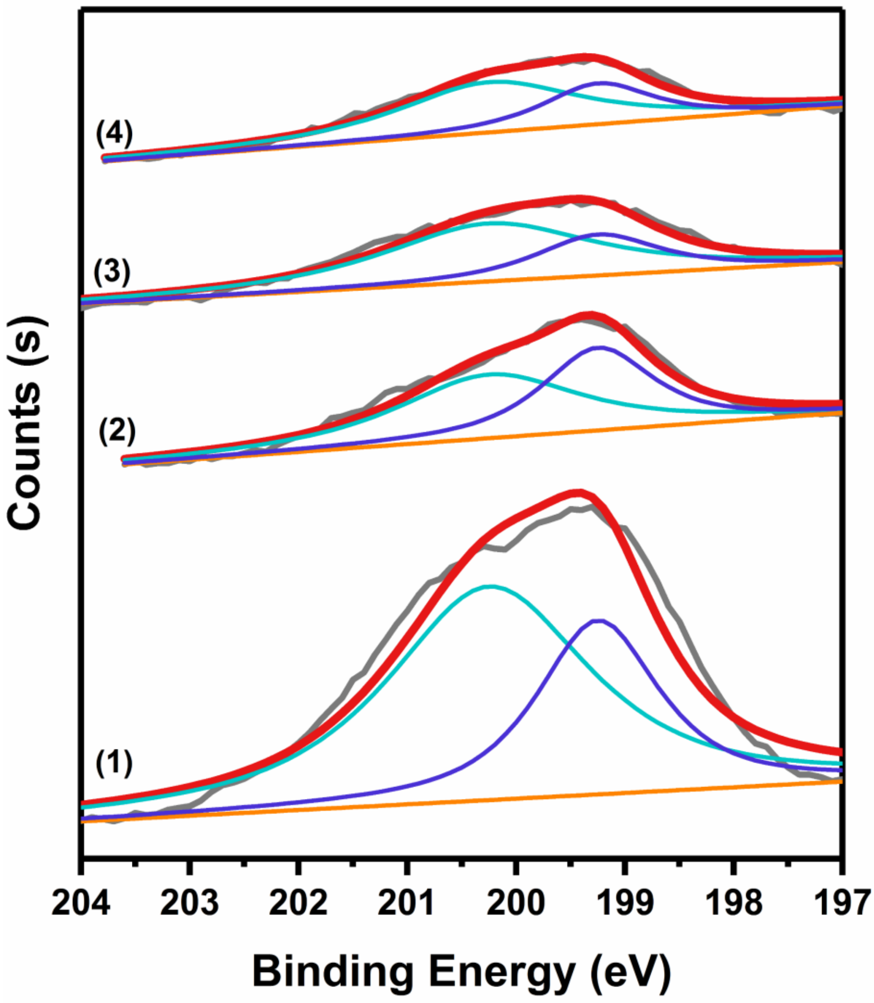

Figure S8. XPS spectrum of Cl 2p for $LaCoO_3$-based catalysts modified with NaCl, (1) fresh 5CuO/$LaCoO_3$-NaCl; (2) spent 5CuO/$LaCoO_3$-NaCl; (3) fresh $LaCo_{0.8}Cu_{0.2}O_{3-\delta}$-NaCl; (4) fresh LaCo0.8Cu0.2$O_{3-\delta}$-NaCl; The concentration of NaCl solution used is 0.0256 M.

XPS of Cl 2p of representative samples were further conducted to illustrate the difference of the Cl variation of 5CuO/$LaCoO_3$-NaCl and $LaCo_{0.8}Cu_{0.2}O_{3-\delta}$-NaCl during the DEP process. But only the data of two kinds of samples (fresh and spent one) were recorded in this study. Cl variation were calculated by the ratio of deconvolution peaks. [2, 3] More information can be obtained in Table S3.

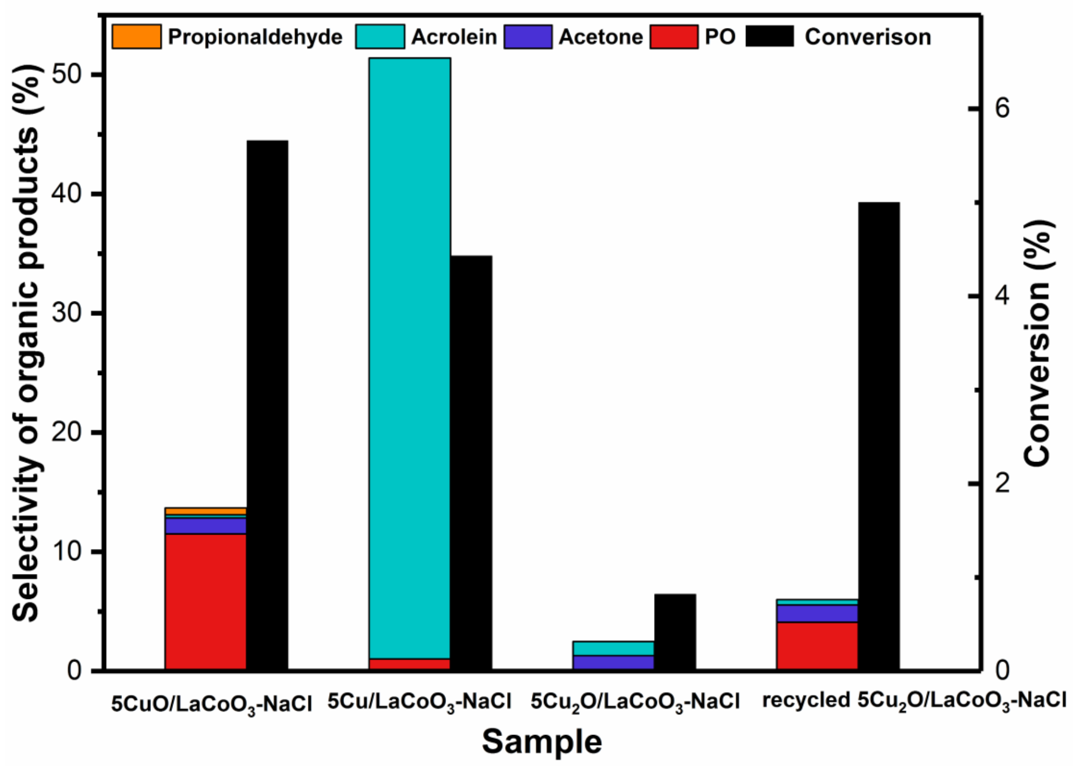

Figure S9. Distribution of organic products over different copper species supported on/$LaCoO_3$-NaCl catalysts and corresponding propylene conversion (The concentration of NaCl solution is 0.0256 M)

Cu/$LaCoO_3$ is prepared by the H_2 reduction of 5CuO/$LaCoO_3$, Cu_2O/$LaCoO_3$ is prepared by a method mentioned in another work,[4] but $LaCoO_3$ is added in the precursor solution in advance. But the existence of Cu^+, Cu^0 in 5CuO/$LaCoO_3$-NaCl catalysts and the oxidation of Cu species in low valence in 5Cu/$LaCoO_3$-NaCl and 5Cu_2O/$LaCoO_3$-NaCl catalysts can not be ignored. The catalytic performance is evaluated under the same reaction conditions.

Table S1. Textural properties of the samples synthesized in this study and previsouly relevant reports for DEP reaction.

Samples	Surface area (m^2/g) [a]	Pore volumn (cm^3/g) [b]	Average Pore size (nm) [c]	Ref.
$LaCoO_3$	5.649	0.019	13.04	This work
$CuO/LaCoO_3$-NaCl	3.519	0.012	38.62	This work
$LaCo_{0.8}Cu_{0.2}O_3$-NaCl	3.033	0.014	17.60	This work
Ag/TiO_2 rutile-NaCl	1.5	0.014	-	[1]
$Ag/CaCO_3$-NaCl	0.9	0.010	-	[1]
CuO_x/SiO_2-$NaNO_3$	465	1.02	7.0	[5]
Cu-modified MoO_3–Bi_2SiO_5/SiO_2	219	0.15	3.43	[6]
$WO_x/Ce_{0.05}Zr_{0.95}O_2$	12.3	-	8.3	[7]

[a] Calculated by the BET (Brunauer–Emmett–Teller) equation

[b] At P/Po =0.99

[c] Obtained from BJH pore size distribution curves

Table S2. Catalytic performance of the samples synthesized in this study and previous works on DEP reaction with molecular oxygen.

No.	Catalyst	Conv.(%)	Sel.(%)	PO yield (%)	Temp. (°C)	Flow rate (mL/min)	Pressure (MPa)	Ref.
1	Cu/SiO_2	1.3	3	0.039	275	50	0.1	[8]
2	NaCl-$VCe_{0.8}Cu_{0.2}$	0.19	43	0.082	250	/	0.1	[9]
3	CuO_x/SBA-15	1	10	0.1	275	60	0.1	[10]
4	K^+–CuO_x /SBA-15	0.48	30	0.15	275	60	0.1	[10]
5	Rhombic dodecahedra Cu_2O	0.8	13	0.10	250	50	0.1	[11]
6	Cubic Cu_2O	0.8	10	0.08	225	50	0.1	[11]
7	Octahedral Cu_2O	0.67	3	0.020	200	50	0.1	[11]
8	Ag-MoO_3 /ZrO_2	0.6	58	0.35	350	62.5	0.1	[12]
9	MoAg/LaSiO_2-NaCl	11.4	17.0	1.94	400	100	0.1	[13]
10	Ag-$CaCO_3$	10	5	0.5	220	30	0.3	[14]
11	NaCl-Ag-$CaCO_3$	3	45	1.35	260	30	0.3	[15]
12	Ag_3/Al_2O_3	/	90	/	100	30	0.13	[16]

13	Ag-$CuCl_2$	1.6	31	0.50	350	60	0.1	[17]
14	Ni-Ag	1.7	11.8	0.20	150	30	0.3	[18]
15	CuO_x/SiO_2-$NaNO_3$	4	13	0.52	350	30	0.1	[5]
16	$Ni_1Ag_{0.4}$ /SBA-15	/	70.7	/	220	20	0.1	[19]
17	$K_{0.02}Fe_{0.005}$ SiO_2	1.4	65	0.91	450	/	/	[20]
18	Ag-Cu-Cl/$BaCO_3$	1.2	83.7	1.00	200	50	0.1	[21]
19	RuO_2–CuO–TeO_2/SiO_2	0.35	47	0.16	269	33	0.1	[22]
20	Ag-Na/$CaCO_3$	11.2	8.2	0.92	350	10	0.2	[23]
21	Ag-ZrO_2-NaCl	13	6.1	0.79	220	50	0.1	[1]
22	Ag-$CuCl_2$ /$BaCO_3$	1.3	71.2	0.93	200	50	0.1	[24]
23	Rhombic dodecahedra Cl-Cu_2O	1.0	63	0.63	200	50	0.1	[2]
24	Rhombic dodecahedra Cl-Cu_2O	0.05	>95	0.048	150	50	0.1	[2]
25	CuO/$LaCoO_3$-NaCl	5.7	11.5	0.66	250	30	0.1	This work
26	$LaCo_{0.8}Cu_{0.2}O_{3-\delta}$-NaCl	12	10.8	1.30	250	30	0.1	This work

Table S3. XPS and AES data (chemical states) of all $LaCoO_3$-based catalysts modified with NaCl (the concentration of NaCl solution is 0.0256 M)

Samples	$Cu^{2+}/(Cu^{+}+Cu^{0})$ [a]	Cu^{0}/Cu^{+} [b]	O_{ele}/O_{latt} [a]	Ratio of deconvolution peaks for Cl 2p [a]	Cl variation (%) [a]
Fresh $5CuO/LaCoO_3$-NaCl	4.85	0.038	3.01	2.03	37.9
Spent $5CuO/LaCoO_3$-NaCl	5.16	0.42	2.27	1.26	
Fresh $LaCo_{0.8}Cu_{0.2}O_{3-\delta}$-NaCl	3.13	1.41	3.09	2.40	15.4
Spent $LaCo_{0.8}Cu_{0.2}O_{3-\delta}$-NaCl	3.15	3.53	2.34	2.03	

[a] calculated by XPS spectrum

[b] calculated by AES spectrum

The ratio of $Cu^{2+}/(Cu^{+}+Cu^{0})$ is based on the peak area of XPS spectrum of Cu 2p. The ratio of Cu^{0}/Cu^{+} is based on the peak area of AES spectrum of Cu LMM.

REFERENCES

(1) Charisteidis, I. D.; Triantafyllidis, K. S., Propylene epoxidation by molecular oxygen using supported silver catalysts: Effect of support type, preparation method and promotion with alkali chloride and/or steam. *Catalysis Today* **2020,** *355*, 654-664.
(2) Zhan, C.; Wang, Q.; Zhou, L.; Han, X.; Wanyan, Y.; Chen, J.; Zheng, Y.; Wang, Y.; Fu, G.; Xie, Z.; Tian, Z. Q., Critical roles of doping Cl on Cu_2O nanocrystals for direct epoxidation of propylene by molecular oxygen. *Journal of the Amreican Chemical Society* **2020,** *142*, 14134-14141.
(3) Wang, Q.; Zhan, C.; Zhou, L.; Fu, G.; Xie, Z., Effects of Cl^- on Cu_2O nanocubes for direct epoxidation of propylene by molecular oxygen. *Catalysis Communications* **2020,** *135*, 1-14.
(4) Zhan, G., Synthetic architecture of integrated nanocatalysts with controlled spatial distribution of metal nanoparticles. *Chemical Engineering Journal* **2019,** *355*, 320-334.
(5) Teržan, J.; Djinović, P.; Zavašnik, J.; Arčon, I.; Žerjav, G.; Spreitzer, M.; Pintar, A., Alkali and earth alkali modified CuO_x/SiO_2 catalysts for propylene partial oxidation: What determines the selectivity? *Applied Catalysis B: Environmental* **2018,** *237*, 214-227.
(6) Wang, Z.; Gao, A.; Chen, P.; Hu, H.; Huang, Q.; Chen, X., The construction of $Mo_{6-\delta}O_{3-x}$-supported catalyst for low-temperature propylene gas-phase epoxidation by Cu modification. *Journal of Catalysis* **2018,** *368*, 120-133.
(7) Lee, E. J.; Lee, J.; Lee, M.; Min, H.-K.; Park, S.; Heui Kim, D., Propylene epoxidation by oxygen over tungsten oxide supported on ceria-zirconia. *Molecular Catalysis* **2019,** *467*, 111-119.
(8) Vaughan, O.; Kyriakou, G.; Macleod, N.; Tikhov, M.; Lambert, R., Copper as a selective catalyst for the epoxidation of propene. *Journal of Catalysis* **2005,** *236* (2), 401-404.
(9) Lu, J.; Luo, M.; Lei, H.; Bao, X.; Li, C., Epoxidation of propylene on NaCl-modified $VCe_{1-x}Cu_x$ oxide catalysts with direct molecular oxygen as the oxidant. *Journal of Catalysis* **2002,** *211* (2), 552-555.
(10) Zhu, W.; Zhang, Q.; Wang, Y., Cu(I)-catalyzed epoxidation of propylene by molecular oxygen. *Journal of Physical Chemistry C* **2008,** *112*, 7731-7734.
(11) Hua, Q.; Cao, T.; Gu, X. K.; Lu, J.; Jiang, Z.; Pan, X.; Luo, L.; Li, W. X.; Huang, W., Crystal-plane-controlled selectivity of Cu_2O catalysts in propylene oxidation with molecular oxygen. *Angewandte Chemie International Edition* **2014,** *53* (19), 4856-61.
(12) Jin, G.; Lu, G.; Guo, Y.; Guo, Y.; Wang, J.; Kong, W.; Liu, X., Effect of preparation condition on performance of Ag–MoO_3/ZrO_2 catalyst for direct epoxidation of propylene by molecular oxygen. *Journal of Molecular Catalysis A: Chemical* **2005,** *232* (1-2), 165-172.
(13) Abdel Dayem, H. M.; Al-Shihry, S. S.; Hassan, S. A., Can lanthanum doping enhance catalytic performance of silver in direct propylene epoxidation over $NaMoAg/SiO_2$? *Journal of Rare Earths* **2019,** *37* (5), 500-507.
(14) Lu, J.; Bravosuarez, J.; Takahashi, A.; Haruta, M.; Oyama, S., In situ UV–vis studies of the effect of particle size on the epoxidation of ethylene and propylene on supported silver catalysts with molecular oxygen. *Journal of Catalysis* **2005,** *232* (1), 85-95.
(15) Lu, J.; Bravo-Suárez, J. J.; Haruta, M.; Oyama, S. T., Direct propylene epoxidation

over modified Ag/$CaCO_3$ catalysts. *Applied Catalysis A: General* **2006,** *302* (2), 283-295.
(16) Lei, Y.; Mehmood, F.; Lee, S., Increased silver activity for direct propylene epoxidation via subnanometer size effects. *Science* **2010,** *328*, 224-228.
(17) Luo, M.; Lu, J.; Li, C., Epoxidation of propylene over Ag-CuCl catalysts using air as the oxidant. *Catalysis Letters* **2003,** *86*, 43-49.
(18) Takahashi, A.; Hamakawa, N.; Nakamura, I.; Fujitani, T., Effects of added 3d transition-metals on Ag-based catalysts for direct epoxidation of propylene by oxygen. *Applied Catalysis A: General* **2005,** *294* (1), 34-39.
(19) Yu, B.; Ayvalı, T.; Raine, E.; Li, T.; Li, M. M.-J.; Zheng, J.; Wu, S.; Bagabas, A. A.; Tsang, S. C. E., Enhanced propylene oxide selectivity for gas phase direct propylene epoxidation by lattice expansion of silver atoms on nickel nanoparticles. *Applied Catalysis B: Environmental* **2019,** *243*, 304-312.
(20) García-Aguilar, J.; Cazorla-Amorós, D.; Berenguer-Murcia, Á., K^- and Ca^- promoted ferrosilicates for the gas-phase epoxidation of propylene with O_2. *Applied Catalysis A: General* **2017,** *538*, 139-147.
(21) Zhang, Q.; Guo, Y.; Zhan, W.; Guo, Y.; Wang, L.; Wang, Y.; Lu, G., Gas-phase epoxidation of propylene by molecular oxygen over Ag-Cu-Cl/$BaCO_3$ catalyst: Effects of Cu and Cl loadings. *Chinese Journal of Catalysis* **2017,** *38* (1), 65-72.
(22) Seubsai, A.; Uppala, C.; Tiencharoenwong, P.; Chukeaw, T.; Chareonpanich, M.; Zohour, B.; Noon, D.; Senkan, S., High stability of ruthenium–copper-based catalysts for epoxidation of propylene. *Catalysis Letters* **2017,** *148* (2), 586-600.
(23) Shigeru, S.; Yasuhiro, S.; Tomoyasu, O.; Naotaka, S.; Naohiro, S.; Masahiro, K.; Nobuhiro, K., Gas-phase epoxidation of propylene to propylene oxide on a supported catalyst modified with various dopants. *Catalysts* **2019,** *9* (8), 638-640.
(24) Zhang, Q.; Chai, G.; Guo, Y.; Zhan, W.; Guo, Y.; Wang, L.; Wang, Y.; Lu, G., Gas-phase epoxidation of propylene by molecular oxygen over Ag-$CuCl_2$/$BaCO_3$ catalyst with low $CuCl_2$ doping: Catalytic performance, deactivation and regeneration. *Journal of Molecular Catalysis A: Chemical* **2016,** *424*, 65-76.